Supplementary Materials for

Emergence and Frustration of Magnetism with Variable-Range Interactions in a Quantum Simulator

R. Islam, C. Senko, W. C. Campbell, S. Korenblit, J. Smith, A. Lee, E. E. Edwards, C.-C. J. Wang, J. K. Freericks, C. Monroe*

*Corresponding author. E-mail: monroe@umd.edu

This PDF file includes:

Supplementary Text
Fig. S1
References (*26–28*)

Supplementary Materials

Generating variable-range AFM Ising interactions   The Ising interaction is generated by globally addressing the ions with two off-resonant laser beams at $\lambda = 355$ nm (*21*), intersecting at right angles with wavevector difference $\Delta k = 2\pi\sqrt{2}/\lambda$ along a principal axis of transverse ion motion (*26*). These beams have beatnote frequencies $\nu_{HF} \pm \mu$ which drive stimulated Raman transitions near the upper and lower motional sidebands of transverse motion in order to impart a spin-dependent optical dipole force (*27*). By setting the beatnotes sufficiently far from the sidebands, motional excitations can be made negligible, resulting in a nearly pure spin-spin coupling mediated by the Coulomb interaction (*11*). The effective transverse magnetic field is generated by simultaneously driving a resonant stimulated Raman transition between the spin states with a beatnote frequency ν_{HF} and a phase that is shifted by $\pi/2$ with respect to the mean phase of the sideband fields. The resulting Ising coupling matrix J_{ij} is given by a sum over contributions from each normal mode of collective motion at frequency ν_m,

$$J_{ij} = \Omega^2 \nu_R \sum_{m=1}^{N} \frac{b_{i,m} b_{j,m}}{\mu^2 - \nu_m^2} \tag{S1}$$

where $\nu_R = h/M\lambda^2 = 18.5$ kHz is the recoil frequency associated with the dipole force on a single $^{171}\text{Yb}^+$ ion of mass M, $b_{i,m}$ is the orthonormal component of ion i with mode m, and Ω is the (uniform) single spin flip Rabi frequency, proportional to the laser intensity at each ion. The symmetric detuning μ of the beatnote from the spin-flip transition controls the sign and range of the interactions (*11*). When μ is set larger than the highest (center-of-mass or COM) mode frequency ν_1, every interaction is AFM, and we can empirically approximate Eq. S1 as falling off with distance as a power law $J_{ij} \approx J_0/|i - j|^\alpha$ with $0 < \alpha < 3$ (*9*) and $J_0 \propto 1/N$. While the COM mode mediates a uniform interaction between all pairs of spins, the other modes introduce non-uniformity in the interactions, and effectively reduce the range of AFM interaction. In practice, we control the interaction range by changing the bandwidth of the transverse mode spectrum, achieved by varying the axial confinement of the ions in the Paul trap. The Ising couplings J_{ij} depend not only on the spatial separation $|i - j|$, but also on the

2

site i itself due to the finite size of the system, with $\sim 10\%$ inhomogeneities across the chain. We average over all the couplings between spins separated by a given number of lattice sites to estimate the power law range exponent α in Eq. 2 (*13*).

In the experiment we use global Raman beams each with an optical power of approximately 1W, having horizontal and vertical waists of about 150 μm and 7 μm respectively, to address the ions. This produces a spin-flip Rabi frequency $\Omega \approx 600$ kHz on resonance, with less than 5% inhomogeneity across the chain. We set the beatnote detuning to $\mu \approx \nu_1 + 3\eta\Omega$, where $\eta = \sqrt{\nu_R/\nu_1}$ is the single ion Lamb-Dicke parameter. This keeps the (primarily COM) phonon excitation probabilities sufficiently low for any setting of the range. The typical nearest neighbor Ising coupling is $J_0 \sim 1$ kHz for $N = 10$ spins. In principle, the Ising interaction range can be varied from uniform to dipolar ($0 < \alpha < 3$), but in this experiment the axial frequency was only varied between 0.62 MHz and 0.95 MHz, and given the COM transverse frequency of $\nu_1 = 4.8$ MHz, this results in a range of Ising power-law exponents $0.7 < \alpha < 1.2$, or a variation of the range of interactions between $\xi = 4$ to $\xi = 10$ sites.

Accounting for finite detection efficiency of N-particle correlations   We detect the spin states using spin-dependent fluorescence collected through f/2.1 optics onto an intensified charge-coupled-device (ICCD) camera or a photomultiplier tube (PMT). The spin state $|\uparrow_z\rangle$ fluoresces from the near-resonant detection beam and appears bright, while the spin state $|\downarrow_z\rangle$ scatters little from the off-resonant detection beam and appears dark. The imager has single-site resolution, allowing us to directly measure the two point correlations to probe the AFM order. The spin detection efficiency is the symmetric probability of correctly diagnosing a particular spin state from measurement, and is typically limited by the residual overlaps in the bright and dark flourescence count distribution (*28*).

The detection efficiency for a single spin is observed to be $\epsilon \approx 95\%$ on the ICCD imager, which is lower than the 98% efficiency on the PMT, due to additional electronic and readout noise. For a crystal of $N = 10$ ions, the spatial overlap between the ion images degrades the

detection efficiency even further. To account for this spatial crosstalk, we fit each single shot image in the experiment to a sum of N Gaussians, where N is the number of ions. The center and width of the Gaussians are pre-calibrated from images of all spins prepared in their bright states, with background subtraction from all spins prepared in their dark states. This results in a spread of detection efficiencies between $93 - 97\%$ per spin, depending upon the state of the neighboring spins. The probability of correctly identifying a $N = 10$-body spin state is thus in the range of $\epsilon^N \sim 50 - 75\%$, so we post-process the detected states to improve this value, following the ideas in Ref. (20). The probability of incorrectly assigning an N-qubit state $|i\rangle$ to the actual underlying state $|j\rangle$ is $M_{ij} = (1 - \epsilon)^{\beta_{ij}} \epsilon^{N - \beta_{ij}}$, where β_{ij} is the number of positions that the N-qubit state $|j\rangle$ differs from $|i\rangle$ through bit flips. The observed probability distribution of all 2^N states is then given by $P'_i = \sum_j M_{ij} P_j$, where P_j is the underlying actual distribution of states, which can be obtained by simply inverting the experimentally measured matrix M_{ij} and forming $P_i = \sum_j M_{ij}^{-1} P'_j$. This increases the effective detection fidelity per spin to roughly 97%, similar to that of a single ion with a PMT. Detection errors are included in all the error bars presented, and represent the range of measurements expected from a representative range of detection efficiencies. Some entries of the post-processed probabilities are slightly negative, due to fluctuations in absolute fluorescence levels that impact the values in the matrix M_{ij} during measurement.
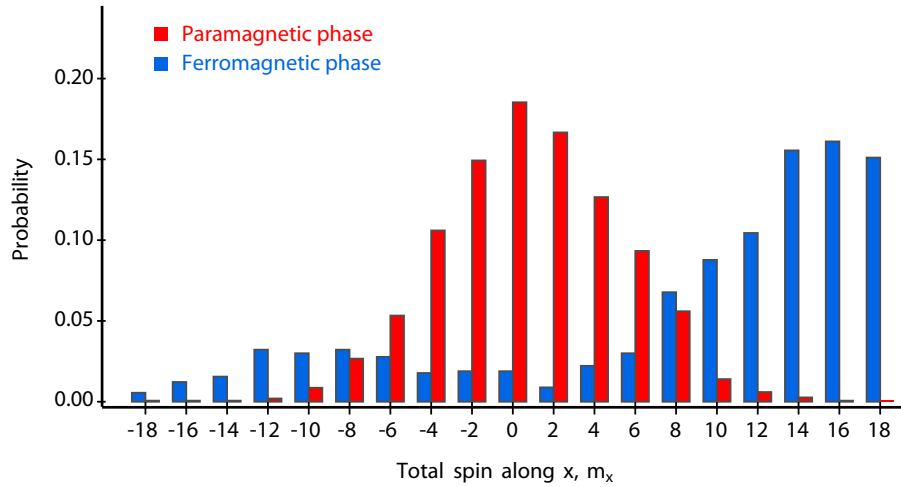
N=18 spin ferromagnetic simulation

Figure S1: Distribution of magnetization in a collection of $N = 18$ spins under the influence of ferromagnetic Ising couplings that fall off as $J_{ij} \sim |i - j|^{-1}$. The paramagnetic phase of the spins is indicated in red, and after the field is ramped to nearly zero, the distribution splits into population weighted heavily towards the FM states $|\downarrow\downarrow\downarrow \cdots \rangle$ and $|\uparrow\uparrow\uparrow \cdots \rangle$, indicated in blue. The resulting magnitude magnetization is approximately $70(10)\%$. The clear bias toward the state $|\uparrow\uparrow\uparrow \cdots \rangle$ may be due to a background effective field along the Ising (axial) direction.

References and Notes

1. H. T. Diep, *Frustrated Spin Systems* (World Scientific, Singapore, 2005).

2. R. Moessner, A. P. Ramirez, Geometrical frustration. *Phys. Today* **59**, 24 (2006). [doi:10.1063/1.2186278](doi:10.1063/1.2186278)

3. S. Sachdev, *Quantum Phase Transitions* (Cambridge Univ. Press, Cambridge, UK, 1999).

4. R. Feynman, Simulating physics with computers. *Int. J. Theor. Phys.* **21**, 467 (1982). [doi:10.1007/BF02650179](doi:10.1007/BF02650179)

5. I. Bloch, J. Dalibard, S. Nascimbéne, Quantum simulations with ultracold quantum gases. *Nat. Phys.* **8**, 267 (2012). doi:10.1038/nphys2259

6. R. Blatt, C. F. Roos, Quantum simulations with trapped ions. *Nat. Phys.* **8**, 277 (2012). doi:10.1038/nphys2252

7. J. Simon *et al.*, Quantum simulation of antiferromagnetic spin chains in an optical lattice. *Nature* **472**, 307 (2011). doi:10.1038/nature09994 Medline

8. G.-B. Jo *et al.*, Ultracold atoms in a tunable optical kagome lattice. *Phys. Rev. Lett.* **108**, 045305 (2012). doi:10.1103/PhysRevLett.108.045305 Medline

9. D. Porras, J. I. Cirac, Effective quantum spin systems with trapped ions. *Phys. Rev. Lett.* **92**, 207901 (2004). doi:10.1103/PhysRevLett.92.207901 Medline

10. A. Friedenauer, H. Schmitz, J. T. Glueckert, D. Porras, T. Schaetz, Simulating a quantum magnet with trapped ions. *Nat. Phys.* **4**, 757 (2008). doi:10.1038/nphys1032

11. K. Kim *et al.*, Entanglement and tunable spin-spin couplings between trapped ions using multiple transverse modes. *Phys. Rev. Lett.* **103**, 120502 (2009). doi:10.1103/PhysRevLett.103.120502 Medline

12. R. Islam *et al.*, Onset of a quantum phase transition with a trapped ion quantum simulator. *Nat. Commun.* **2**, 377 (2011). doi:10.1038/ncomms1374 Medline

13. J. W. Britton *et al.*, Engineered two-dimensional Ising interactions in a trapped-ion quantum simulator with hundreds of spins. *Nature* **484**, 489 (2012). doi:10.1038/nature10981 Medline

14. A. Khromova *et al.*, Designer spin pseudomolecule implemented with trapped ions in a magnetic gradient. *Phys. Rev. Lett.* **108**, 220502 (2012). doi:10.1103/PhysRevLett.108.220502 Medline

15. K. Kim *et al.*, Quantum simulation of frustrated Ising spins with trapped ions. *Nature* **465**, 590 (2010). doi:10.1038/nature09071 Medline

16. E. E. Edwards *et al.*, Quantum simulation and phase diagram of the transverse-field ising model with three atomic spins. *Phys. Rev. B* **82**, 060412 (2010). doi:10.1103/PhysRevB.82.060412

17. S. Olmschenk *et al.*, Manipulation and detection of a trapped Yb^+ hyperfine qubit. *Phys. Rev. A* **76**, 052314 (2007). doi:10.1103/PhysRevA.76.052314

18. See supplementary materials on *Science* Online.

19. K. Binder, Critical properties from Monte Carlo coarse graining and renormalization. *Phys. Rev. Lett.* **47**, 693 (1981). doi:10.1103/PhysRevLett.47.693

20. C. Shen, L.-M. Duan, Correcting detection errors in quantum state engineering through data processing. *New J. Phys.* **14**, 053053 (2012). doi:10.1088/1367-2630/14/5/053053

21. W. C. Campbell *et al.*, Ultrafast gates for single atomic qubits. *Phys. Rev. Lett.* **105**, 090502 (2010). doi:10.1103/PhysRevLett.105.090502 Medline

22. C.-C. J. Wang, J. K. Freericks, Intrinsic phonon effects on analog quantum simulators with ultracold trapped ions. *Phys. Rev. A* **86**, 032329 (2012). doi:10.1103/PhysRevA.86.032329

23. R. Moessner, S. L. Sondhi, Ising models of quantum frustration. *Phys. Rev. B* **63**, 224401 (2001). doi:10.1103/PhysRevB.63.224401

24. A. W. Sandvik, Ground states of a frustrated quantum spin chain with long-range interactions. *Phys. Rev. Lett.* **104**, 137204 (2010). doi:10.1103/PhysRevLett.104.137204 Medline

25. Quantum Monte Carlo algorithms can be used to calculate static equilibrium properties of the transverse field Ising model for large numbers of interacting spins, so ground states and static correlation functions can indeed be calculated for large systems (*23*). However, the calculation of dynamics and nonequilibrium behavior of quantum spin models is not currently feasible for these Monte Carlo approaches, and in the presence of frustrated long-range interactions, the general behavior of such systems requires exact diagonalization. Other techniques such as the density matrix renormalization group become too difficult with long-range interactions. Because the size of the Hilbert space grows exponentially with the number of spins, sparse-matrix techniques such as the Lanczos method must therefore be used. Current state-of-the-art work on such systems is limited to sizes on the order of 30 to 35 spins (*24*).

26. S.-L. Zhu, C. Monroe, L.-M. Duan, Trapped ion quantum computation with transverse phonon modes. *Phys. Rev. Lett.* **97**, 050505 (2006). doi:10.1103/PhysRevLett.97.050505 Medline

27. D. Leibfried, R. Blatt, C. Monroe, D. Wineland, Quantum dynamics of single trapped ions. *Rev. Mod. Phys.* **75**, 281 (2003). doi:10.1103/RevModPhys.75.281

28. M. Acton *et al.*, Near-perfect simultaneous measurement of a qubit register. *Quant. Inf. Comp.* **6**, 465 (2006).